

temperature distribution. However, the cited results pertain to that initial stage of the process in which the heating is still small. According to formula (2.5), the temperature difference across the cross section amounts approximately to 2 K; with an initial temperature of 18 K the relationship between the properties and temperature in this case is not apparent [1].

LITERATURE CITED

1. M. Wilson, Superconductive Solenoids [Russian translation], Mir, Moscow (1985).
2. I. E. Tamm, Fundamentals in the Theory of Electricity [in Russian], Nauka, Moscow (1975).
3. N. M. Belyaev and A. A. Ryadno, Methods in the Theory of Heat Conduction [in Russian], Vysshaya Shkola, Moscow (1982).
4. A. I. Lur'e, The Theory of Elasticity [in Russian], Nauka, Moscow (1970).
5. V. Novacky, Electromagnetic Effects in Solids [Russian translation], Mir, Moscow (1986).

THE DYNAMICS OF AIR FLOW IN THE PRESENCE OF AN ENERGY PULSE IN THE SPHERICAL REGION, WITH PROVISION MADE FOR VIBRATIONAL-TRANSLATIONAL NONEQUILIBRIUM

A. Kh. Mnatsakanyan, G. V. Naidis, and S. V. Rumyantsev

UDC 533.9

Numerous papers have been devoted to questions dealing with the dynamics of a gas in the presence of energy sources. We are thoroughly familiar with solutions to problems dealing with a powerful point explosion and with a spot explosion in which consideration is given to the counterpressure in an ideal gas with a constant adiabatic exponent for cases of plane, cylindrical, and spherical symmetry [1, 2]. Such explosions are similar to one another, if the variables are normalized to the corresponding parameters ρ_∞ , p_∞ of the unperturbed gas, as well as to the characteristic dimensions and times of attenuation for the explosion wave, i.e., $r_0 = (E_0/p_\infty)^{1/n}$, $\tau_0 = r_0(\rho_\infty/p_\infty)^{1/2}$ (E_0 is the energy released per unit area or length, or the total energy of the explosion, $n = 1, 2, 3$ for plane, cylindrical, and spherical symmetry). The solution from point explosion theory (PET) frequently provides a good relationship for the magnitudes of the jumps in the gasdynamic variables at the front of the shock wave (SW) at great distances from the center of the explosion (when $r \gg R_0$, R_0 is the radius of the energy-release zone). However, in order to examine the distribution of the gasdynamic quantities over small periods of time, as well as to examine the finite distribution of temperature in the region of energy release after equalization of the pressure it is necessary to take into consideration the finiteness of the dimensions of the energy-release region and the time over which the energy contribution is effective.

The release of energy in a gas frequently comes about in nonequilibrium fashion. Thus, in a pulsed electric discharge in a molecular gas the greater portion of the released energy is stored in the vibrational degrees of molecular freedom, which leads to a significant divergence of the vibrational energy from equilibrium. In this case, in our analysis of the gasdynamic phenomena, we have to examine the kinetics of the exchange of energies between the internal and translational degrees of freedom for the molecules. The gasdynamics of nonequilibrium excited nitrogen was examined for instances of plane and cylindrical symmetry in [3, 4]. The duration of the excitation pulse was assumed, in this case, to be infinitely small.

The gasdynamic phenomena in the nonequilibrium excitation of the spherical region in air is examined in this study for various ratios of the time τ of the energy contribution and the characteristic gasdynamic and relaxation times.

With a given initial gas temperature T_∞ , a specific (per unit mass) applied energy Q , and its fraction ξ stored in the vibrational degrees of freedom, the nature of the gas flow is determined by two dimensionless quantities, the ratios of the above-indicated three characteristic times. Since the relaxation time $\tau_V \sim p_\infty^{-1}$, and the gasdynamic time $\tau_x \sim R_0$ (to the radius of the energy-release zone), the similarity parameters in this problem are $p_\infty R_0$ and R_0/τ . The calculations were carried out for $p_\infty R_0 = 10^3, 10^4, \text{ and } 10^5 \text{ Pa}\cdot\text{m}$, $R_0/\tau = 10^3$ and $2 \cdot 10^4 \text{ m/sec}$ for $T_\infty = 300 \text{ K}$, $Q = 1.1 \cdot 10^6 \text{ J/kg}$ (which corresponds to $\sim 0.33 \text{ eV/molecule}$), $\xi = 0.77$. The quantities Q and ξ are typical for the conditions of excitation for the air by means of a pulsed high-frequency charge [5].

The system of one-dimensional nonstationary gasdynamics equations in Lagrange mass variables for spherical-symmetric flow was solved numerically for the times $t > 0$:

$$\begin{aligned} \frac{\partial v}{\partial t} &= -r^2 \frac{\partial p}{\partial s}, \quad \frac{\partial r}{\partial t} = v, \quad \eta = \frac{\partial r^3}{\partial s}, \\ \frac{\partial \varepsilon}{\partial t} &= -p \frac{\partial}{\partial s} (r^2 v) + \frac{Q}{\tau} \theta(\tau - t) \theta(s_0 - s), \quad \varepsilon = \varepsilon_V^{N_2} + \varepsilon_V^{O_2} + \frac{\eta p}{\gamma - 1}. \end{aligned} \quad (1)$$

Here v is the velocity; p , pressure; ε , total specific internal energy (per unit mass of the gas); s , the Lagrange mass variable, equal to the mass of gas per unit solid angle (the value of $s = s_0$ corresponds to the initial distance $r = R_0$); γ , the adiabatic exponent (for air $\gamma = 1.4$); η , the specific volume; $\varepsilon_V^{N_2}$ and $\varepsilon_V^{O_2}$, respectively, the specific vibrational energies of nitrogen and oxygen; $\theta(x) = 0$ when $x < 0$ and 1 for the case in which $x \geq 0$. System (1) was enhanced with the relaxation equation for the vibrational energy of N_2 ($\varepsilon_V^{O_2}$ was assumed at each instant to be equal to its equilibrium value, determined by the translational temperature of the gas)

$$\frac{\partial \varepsilon_V^{N_2}}{\partial t} = -\frac{\varepsilon_V^{N_2} - \varepsilon_V^{N_2_0}}{\tau_V} + \frac{\xi Q}{\tau} \theta(\tau - t) \theta(s_0 - s) \quad (2)$$

($\varepsilon_V^{N_2_0}$ is the equilibrium value of $\varepsilon_V^{N_2}$). The time τ_V of the vibrational relaxation of N_2 is determined from an expression approximating the calculation results from [6]:

$$(\tau_V n_m)^{-1} = \left[\frac{A_1 \zeta_{H_2O}}{1 - \exp(-\omega_{H_2O}/T)} + \frac{A_2}{1 - \exp(-\omega_{O_2}/T)} \right] (1 - \exp(-\omega_{N_2}/T)) + A_3 q_{N_2}^2 \text{ (m}^3/\text{sec)}, \quad (3)$$

where n_m is the total molecule concentration; $\zeta_{H_2O} = n_{H_2O}/n_m$ is the molar fraction of the water vapors (assumed in the calculations to be equal to 0.01); ω_{H_2O} , ω_{O_2} , ω_{N_2} are the vibrational quanta of H_2O (the vibrational mode ν_2), O_2 and N_2 in K; $A_1 = 1.5 \cdot 10^{-13} \exp(-96.1/T^{1/2})$, $A_2 = 1.1 \cdot 10^{-24} T^{3/2} \cdot \exp(-156/T^{1/2})$, $A_3 = 3.1 \cdot 10^{-28} T^2$; q_{N_2} is the average number of vibrational quanta per single nitrogen molecule. The terms in the brackets in (3) correspond to the extinction of the N_2 vibrations by O_2 and H_2O molecules. The last term in (3) makes provision for the effects of anharmonicity.

System of equations (1), (2) was solved numerically by means of a difference method with the aid of an implicitly totally conservative difference scheme, described in detail in [7], involving the use of a grid uniform with respect to the Euler coordinate. The calculation of the SW is accomplished in direct fashion, by using the Neumann artificial viscosity [7].

The calculated pressure profiles for the case of short pumping pulses ($R_0/\tau = 2 \cdot 10^4 \text{ m/sec}$) are shown in Fig. 1. Figure 1a shows the results corresponding to $p_\infty R_0 = 10^5 \text{ Pa}\cdot\text{m}$ for the instants of time $t/\tau_x = 0.21, 0.42, 0.62, 0.83, 0.92, 1.09, \text{ and } 1.32$ (lines 1-7, $\tau_x = R_0/a$, a is the speed of sound in the unperturbed gas). In this case both the duration of the pulse and the time of the vibrational relaxation of N_2 are smaller than the gasdynamic time τ_x , then the transition of all the energy applied to the translational degrees proceeds isochorically and the pattern of the flow turns out to be analogous to that calculated in [8], where we find an examination of the process of the disintegration of the spherical region with elevated pressure and temperature. The SW and the refraction waves begin to propagate from the boundaries of the region of energy release. On reaching the center of the sphere, the rarefaction wave sharply reduces both pressure and density there, so that a significant pressure gradient is developed from the periphery to the center. Under the action of this pressure gradient the gas particles that are not overly close to the front

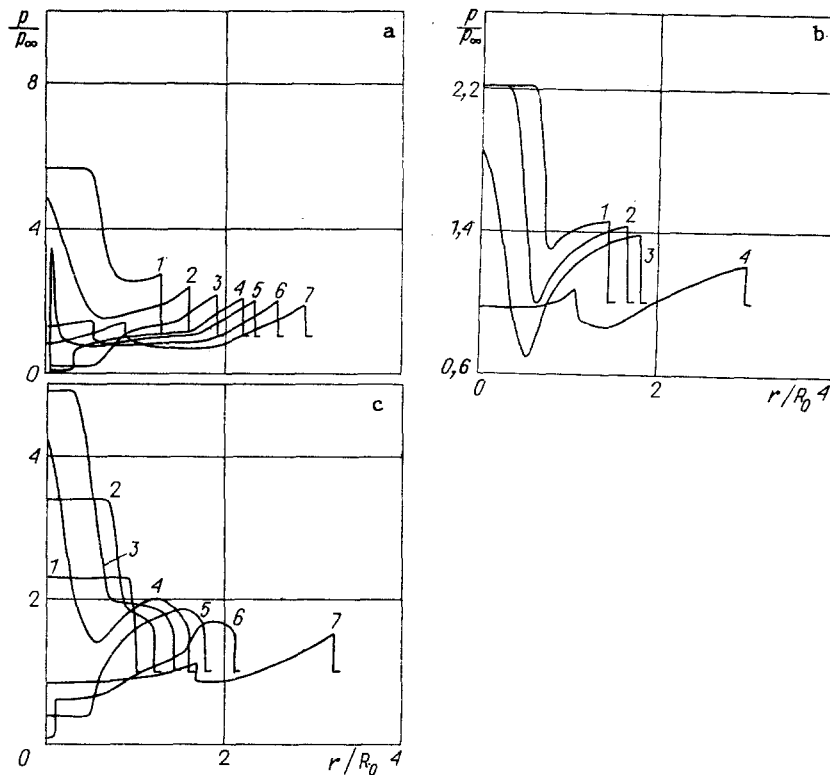


Fig. 1

of the SW, moving initially from the center, are decelerated and at some instant of time their velocity changes sign. SW are formed, converging on the center. Collapsing in the direction of the center of the sphere and being reflected from that center, the wave markedly heats the central region. The reflected wave forms a second front in the explosion wave, which is thus converted into an N-shaped wave (the so-called N-wave). The characteristic dimensions between the pressure discontinuities in the N-wave at the instant of its formation amounts to $\sim 2R_0$ and grows only weakly over time.

Figure 1b shows the pressure profiles for the case in which $p_{\infty}R_0 = 10^3$ Pa·m for the times $t/\tau_* = 0.35, 0.52, 0.62,$ and 1.74 (lines 1-4). In this case $\tau_V \gg \tau_*$, as a result of which the N-wave forms only due to the direct heating; the vibrational relaxation occurs isobarically. The pressure profiles for the intermediate value of $p_{\infty}R_0 = 10^4$ Pa·m are shown in Fig. 1c for $t/\tau_* = 0.035, 0.17, 0.35, 0.49, 0.62, 0.83,$ and 1.74 (lines 1-7). Here the disintegration proceeds simultaneously with the relaxation of the vibrations in N_2 . The rarefaction wave propagates within the energy-release region simultaneously with the rise in pressure in the central region. We can see that unlike the above-cited cases of SW formation we have a nonmonotonic pressure profile in the initial stage, and this profile, consequently, changes into an ordinary N-shaped profile with a monotonic drop in pressure behind the front.

Calculations were also carried out for an extended period of energy input with $R_0/\tau = 10^3$ m/sec (for $\tau_*/\tau = 2.9$). The basic outlines of the disintegration process are analogous

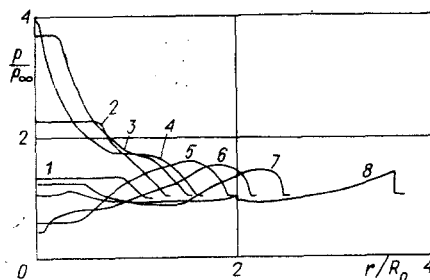


Fig. 2

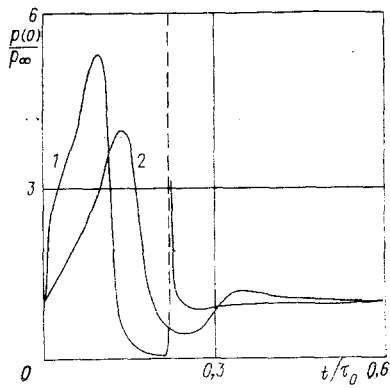


Fig. 3

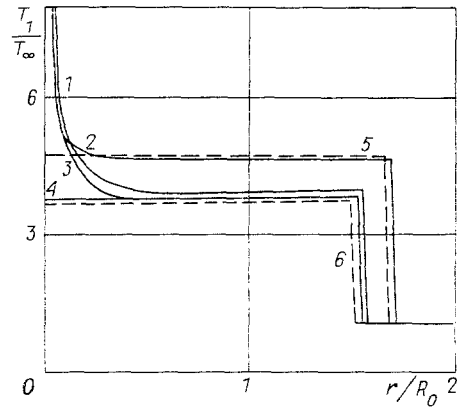


Fig. 4

to the case with small τ examined above. The parameters of the resulting SW coincide approximately, as does the relationship between the SW and distance. However, with a prolonged pumping pulse no return SW is formed and therefore no strongly heated region near the center is formed. As can be seen in Fig. 2, which shows the pressure profiles for $p_{\infty}R_0 = 10^4$ Pa·m, $R_0/\tau = 10^3$ m/sec for $t/\tau_{*} = 0.10, 0.31, 0.52, 0.62, 0.94, 1.15, 1.46,$ and 2.6 (lines 1-8), the formation of the leading SW does not occur instantaneously (unlike the case of rapid pumping, see Fig. 1c) and concludes approximately at the instant $t/\tau_{*} = 1.5$. The difference between the versions with slow and rapid pumping is also illustrated in Fig. 3, in which we find the time relationships of pressure at the center of the energy-release region for regimes corresponding to Fig. 1c and Fig. 2 (lines 1 and 2), expressed in units of PET (see above). We see that with a short pumping pulse the relationship is more pronounced in nature. After a rapid drop in pressure, resulting from the arrival of rarefaction wave, we have a burst from the return SW, which is then followed by a constant external pressure.

The final profiles of temperature and density (after the pressure has been made equal to the external pressure in the energy-release region) for the thermal nonuniformity were found by recalculating the parameters of the region, after the second front of the N-wave has departed from that region, by means of the following formulas:

$$T_1(s) = T(s)(p_{\infty}/p(s))^{1-1/\gamma}, \quad \eta_1(s) = \eta(s)(p(s)/p_{\infty})^{1/\gamma}, \quad r_1(s) = \left(3 \int_0^s \eta_1(s) ds \right)^{1/3},$$

where s is the Lagrange coordinate; $r_1(s)$, the finite distance from the center to the gas particle with coordinate s ; $p(s)$, $T(s)$, $\eta(s)$, the initial profiles of pressure, temperature, and specific volume. These formulas correspond to the adiabatic expansion or compression of the gas particle with the parameters $p(s)$, $\eta(s)$ to the pressures p_{∞} [9].

Figure 4 shows the profiles of the finite temperature for the conditions corresponding to Fig. 1a-c and Fig. 2 (lines 1-4). We can see that the region of strongly heated gas near the center exists only in the case of rapid energy input. Here we also find the profiles of the finite temperature for characteristic energy-release regimes: isobaric and isochoric, with subsequent adiabatic expansion (lines 5 and 6). It is easy to show that the finite temperature in the isobaric regime is expressed by $T_1/T_{\infty} = 1 + (\gamma - 1)Q/(\gamma RT_{\infty})$, while in the case of the isochoric-adiabatic regime $T_1/T_{\infty} = (1 + (\gamma - 1)Q/(RT_{\infty}))^{1/\gamma}$ (R is the gas constant, and for air $R = 289$ J/kg/K). The finite dimension of the energy-release region for these cases is obviously $R_1 = R_0(T_1/T_{\infty})^{1/3}$. We can see from Fig. 4 that the finite temperature profiles for $p_{\infty}R_0 = 10^4$ and 10^5 Pa·m are close to the profile for the isochoric-adiabatic regime of energy release, while for $p_{\infty}R_0 = 10^3$ Pa·m they are close to the relationships for the isobaric regime of energy release.

The calculations which we have carried out have demonstrated the significant influence of nonequilibrium in energy release (with $p_{\infty}R_0 \leq 10^4$ Pa·m) and the duration of pumping on the nature of the gas flow. We have determined the intensity of the formed SW as a function of the distance to the center of the region of energy release in the case of typical values for the specific energy input under conditions of a pulsed electric discharge.

LITERATURE CITED

1. L. I. Sedov, *The Methods of Similarity and Dimensionality in Mechanics* [in Russian], Nauka, Moscow (1981).
2. V. P. Korobeinikov, *Problems in the Theory of a Spot Explosion* [in Russian], Nauka, Moscow (1985).
3. T. E. Andreeva, S. I. Gritsinin, I. A. Kosygi, et al., "Relaxation of vibrationally excited nitrogen with consideration of gasdynamics phenomena," *Brief Communications in Physics*, No. 7 (1983).
4. V. A. Gasilov, V. Ya. Karpov, A. Yu. Krukovskii, et al., "Calculating the development of an axisymmetric thermal explosion in a molecular gas," *Preprint, IVTAN*, No. 5-138, Moscow (1984).
5. A. L. Vikharev, M. S. Gitlin, O. A. Ivanov, et al., "The heating of nitrogen in a pulsed SHF discharge under conditions of intensive excitation of molecular electron levels," *Pis'ma Zh. Tekh. Fiz.*, 13, No. 4 (1987).
6. A. Kh. Mnatsakanyan and G. V. Naidis, "Difference methods for the solution of gasdynamic problems," *Teplofiz. Vys. Temp.*, 23, No. 4 (1985).
7. A. A. Samarskii and Yu. P. Popov, *Difference Methods of Solution of Gasdynamic Problems* [in Russian], Nauka, Moscow (1980).
8. H. Honma and I. I. Glass, "Weak spherical shock-wave transitions of N-waves in air with vibrational excitation," *Proc. R. Soc. London*, A391, No. 1800 (1984).
9. Ya. B. Zel'dovich and Yu. P. Raizer, *The Physics of Shock Waves and High-Temperature Hydrodynamic Phenomena* [in Russian], Nauka, Moscow (1966).

THE FORMATION OF SHOCK WAVES WITH AN EXPLOSIVE PROFILE IN A SHOCK TUBE

M. K. Berezkina, I. V. Smirnov, and M. P. Syschchikova

UDC 533.6.011.72:534.222.2

A plane shock wave (SW) with a variable pressure profile behind the front can be produced in a shock tube of constant cross section, with a diaphragm, at the point at which the SW front overtakes the rarefaction wave (RW), reflected from the end of a high-pressure chamber (HPC).

Based on a numerical model of the flow which occurs in the explosion of a layer which can be represented as a flow that is achieved in a shock tube in the case of the instantaneous removal of the diaphragm, it has been demonstrated in [1] that there exists such values of the determining parameters that the pressure at the front of the SW at the instant at which the head of the RW is overtaken is close to the pressure at the front of the SW in the case of a point plane explosion. Further changes in the pressure at the front of the SW are also close to the relationship between the pressure at the front of the SW and the distance for the point explosion. Given other values for the determining parameters, the pressure at the front of the SW at the instant of overtaking the RW is smaller than the pressure of the point explosion and approach to the quantitative relationship governing the point explosion occurs at a distance exceeding the distance required to overtake the other wave.

At the present time the model of the point explosion has been studied more thoroughly [2] and in many cases provides an excellent description of the problem of real explosions. The interrelationship of the parameters of a SW formed in a shock tube after the RW has been overtaken with the parameters of the SW in the case of a point explosion, such as observed in numerical modeling [1], is deserving of attention. We have the possibility of using installations of this kind to model the processes of interaction between bodies and the waves from an explosion.

Leningrad. Translated from *Zhurnal Prikladnoi Mekhaniki i Tekhnicheskoi Fiziki*, Vol. 30, No. 6, pp. 50-56, November-December, 1989. Original article submitted July 15, 1988.